Appendix

The high-energy transition state of a membrane transporter

Gerard H. M. Huysmans[1,2,*], Didar Ciftci[1,3], Xiaoyu Wang[1], Scott C. Blanchard[1,3,4], Olga Boudker[1,3,5,*]

Table of Content

Appendix Tables

Appendix Table S1: Global difference scores (GDS) of amino acid positions with significant distribution changes. *Related to Figure 1.*

AA in Glt_{Ph}	AA position	GDS volume	GDS physicochemical properties	AA in meso/psychrophile	Structural location
L	13	0.35			TM1
Q	14	0.78	0.35		TM1/exposed
I	21		0.21		TM1/exposed
V	39	0.01			TM1-2 loop
S	65	0.80		T	TM2/TD-scaffold interface
A	70	0.38		I	Intracellular hinge
S	74	0.59			Intracellular hinge
V	87		0.94		TM3/exposed
Y	89		0.09		TM3/binding
T	92	0.06			TM3/core TD
A	94	1.41		T/L/I/F	TM3/HP2 packing
V	97	1.31	0.55	L/I	TM3/HP2 packing
R	105	0.11			TM3/exposed
I	113	0.49			TM3-4 loop
A	127	0.06			TM3-4 loop
P	128	0.32	1.14		TM3-4 loop
P	153	0.25	0.75		TM4
I	165	0.19			TM4
G	189	0.19			TM5/exposed
A	193	1.05			TM5/exposed
N	199		0.05		TM5/exposed
A	211		0.02		TM5
V	231		0.02		TM6
T	232	0.20			TM6
A	234	0.07			TM6
V	235	0.84		F/L	TM6
V	237		0.10		TM6/exposed
Q	242	1.35	0.42	F/L/I/V	TM6
I	243	0.62			TM6/exposed
K	254	0.28			TM6/exposed
G	255		0.25		TM6-HP1 loop
P	258	0.46			TM6-HP1 loop
A	265	0.48	0.41	I/L/M	HP1
A	268	1.17	0.58	E/V	HP1

M	269		0.69	Q/A/G/S/T	HP1
T	271	0.66	0.11	L/I/F/V	HP1
S	279	0.31			HP1 tip
T	281		0.40	V/A	HP1
V	284		0.57	L/R/K	HP1
T	285	0.15		L/I/M/V	HP1
V	288	0.02	0.42	K/T/A	HP1
K	289	1.10	0.51	L/M/V	HP1
M	292	0.92	0.02		HP1-TM7 loop/exposed
A	307	1.41	0.42		TM7/binding
Q	318	0.44	0.37	L/I/P	TM7/HP2 packing
G	319	0.17		T/S	TM7/HP2 packing
V	320	0.13			TM7
G	330	0.22			TM7-HP2 loop/exposed
T	344	0.98		V/I	HP2
A	345	1.12	0.31	L/S/V	HP2
V	346	0.38	0.07	T/M/L/I	HP2
A	348	0.22	0.28	T/S	HP2
P	356		0.10		HP2 tip
V	366	0.39		T/A	HP2
S	369	1.17		Q/V/L/M	HP2
V	370	0.27			HP2
D	405		0.57		TM8/binding
L	406		0.41	A/S/C	TM8/HP1 packing
G	408	0.46	0.50	A/V	TM8
T	409	0.47	0.45		TM8
T	415		0.00		TM8/exposed

The shading is according to the structural regions, as in Figure 1.

Appendix Table S2: Kinetic parameters of ^{3}H-L-Asp uptake by Glt$_{Ph}$ variants. *Related to Figure 1.*

Glt$_{Ph}$ variant	K_M[a]	Fold rate change[a]
WT	0.50 ± 0.04	(average rate 0.06 ± 0.05 s^{-1})[b]
HP1 substitutions		
A265L	0.42	1.4[c]
A265M	0.34	1.4
A265V	0.55	0.6
A268V	0.30 ± 0.08	0.7 ± 0.5
M269A	0.59 ± 0.27	1.7 ± 0.5
M269V	0.77	1.6
M269Q	0.11	1.5
M269L	0.37	0.5
T285V	0.34 ± 0.02	1.8 ± 0.3
A289L	1.28	1.0
HP2 substitutions		
I341A	0.27	0.4
A345V	**0.79 ± 0.28**	**4.0 ± 1.2**
A345S	**0.84**	**3.8**
A345L	0.70	0.5
A345F	0.42	0.3
V346T	0.25	0.7
M362V	**1.11**	**7.9**
V366A	**2.82 ± 1.11**	**6.8 ± 4.1**
V366T	0.53	1.0
Scaffold substitutions		
D48N	0.33	2.0
A70I	0.31 ± 0.23	0.8 ± 0.3
P75G	0.29	1.0
A191N	0.10	0.5
Y195F	0.58	0.6
Y204L	**0.48 ± 0.26**	**3.7 ± 1.6**
Y204V	0.39	1.0
Y204F	0.45	0.7
Q220A	N.D.[d]	N.D.[d]
H223D	1.49	2.0
G226L	0.55 ± 0.72	1.9 ± 0.3
E227G	0.73	0.2
Transport domain core substitutions		
I85A	0.25	1.5
A94T	0.48	0.7
V97I	3.01	3.0
V97A	0.33	0.9
V235F	0.50	1.9
Q242F	0.14 ± 0.10	0.4 ± 0.1
L303A	0.29	1.2
L303V	0.31	0.3
Q318L	0.38	1.5
T322A	0.95	0.8
L406A	0.15	0.6
G408A	0.45	0.4

Combination variants		
A345V V366A	**1.56 ± 0.40**	**11.1 ± 5.9**
Y204L A345V V366A	**1.61 ± 0.42**	**12.7 ± 2.5**
D48A Y204L	0.43	2.2
V366A Y204L	1.29 ± 0.69	5.1 ± 5.2
A345V Y204L	1.38 ± 0.60	3.0 ± 1.0
V366A G226L	12.55	5.2
V366A Y204L G226L	0.97	9.1
A345V G226L V366A	1.48	3.3
V366A A345V A70I	4.35	8.0
A265M L406A V288T A289L	0.62	1.0
A345V A265M	0.83	3.0
Y204L A265M	1.09	4.3
V366A A265M	1.57	2.6
V366A Y204L A265M	0.92	6.0
V366A A345V M269A	2.56	3.3
V366A A345V A289L	5.99	2.7
V366A A345V Y204L A268V	5.20	8.6
V366A A345V A265M	2.15 ± 1.54	11.0 ± 7.8
V366A Y204L A345V M269A	2.1	14.0
V366A A345V Y204L A265M L406A V288T A289L	N.D.[d]	N.D.[d]
V366A A345V Y204L A265M	3.1	3.8
V366A A345V A265M G226L	1.49	3.3
V366A A345V A265M A70I	2.14	3.3
Combinations containing K290A or R276S M395R		
R276S	0.76	2.2
K290A	**0.41 ± 0.11**	**1.7 ± 1.2**
R276S M395R	**1.33 ± 1.16**	**8.0 ± 3.2**
V366A A345V Y204L K290A	**2.64 ± 1.41**	**17.7 ± 0.9**
R276S M395R V366A Y204L A345V	N.D.[d]	N.D.[d]
R276S M395R V366A	4.12	4.0
K290A Y204L	**0.38 ± 0.17**	**2.6 ± 0.6**
K290A A345V V366A	**0.61 ± 0.15**	**9.4 ± 4.4**
K290A Y204L A268V A345V V366A	5.12	8.2
R276S Y204L A265M A345V V366A	N.D.[d]	N.D.[d]
R276S Y204L M269A A345V V366A	0.88	3.3
R276S M395R Y204L M269A A345V V366A	N.D.[d]	N.D.[d]
R276S M395R Y204L G226L A345V V366A	N.D.[d]	N.D.[d]
R276S M395R Y204L M269A L303A A345V V366A	N.D.[d]	N.D.[d]

[a] values obtained by fitting data to the Michaelis-Menten equation. When shown, errors are standard deviations for at least three independent experiments. When errors are not shown, experiments were only performed once.
[b] from 34 independent experiments.
[c] fold change of initial rate relative to the WT transporter tested on the same day.
[d] not determined because poor transport rates preclude analysis.

Appendix Table S3: Glt_{Ph} dynamics in the presence of the non-transportable inhibitor DL-TBOA. *Related to Figure 3.*

Glt_{Ph} variant	transition frequency (s^{-1})	Number of molecules	% of molecules containing 90% of measured transitions
WT	0.03 ± 0.01	1287	8
Y204L	0.02 ± 0.01	1282	16
G226L	0.06 ± 0.02	1298	10
M269A	0.03 ± 0.01	1637	10
A345V	0.03 ± 0.02	1727	12
V366A	0.03 ± 0.01	1403	16
A345V V366A	0.03 ± 0.01	1678	10
Y204L A345V V366A	0.03 ± 0.01	1586	16
K290A	0.06 ± 0.03	1933	13
K290A Y204L	0.10 ± 0.02	894	17
K290A A345V V366A	0.02 ± 0.02	1067	13
K290A Y204L A345V V366A	0.04 ± 0.03	1498	13
R276S M395R	0.04 ± 0.01	742	12

Appendix Table S4: X-ray crystallographic data and refinement statistics for the Y204L/A345V/V366A Glt_{Ph} structure deposited to the PDB. *Related to Figure 3.*

Wavelength	0.99997
Resolution range	47.38 - 3.375 (3.496 - 3.375)
Space group	P 31 2 1
Unit cell	109.416 109.416 305.227 90 90 120
Total reflections	321457 (22766)
Unique reflections	30612 (2964)
Multiplicity	10.5 (7.7)
Completeness (%)	99.54 (98.40)
Mean I/sigma(I)	10.87 (1.87)
Wilson B-factor	114.03
R-merge	0.1155 (1.074)
R-meas	0.1212 (1.153)
R-pim	0.03574 (0.4091)
CC1/2	0.993 (0.787)
CC*	0.998 (0.939)
Reflections used in refinement	30565 (2956)
Reflections used for R-free	1400 (156)
R-work	0.2324 (0.3367)
R-free	0.2574 (0.3916)
CC(work)	0.818 (0.835)
CC(free)	0.854 (0.667)
Number of non-hydrogen atoms	8679
macromolecules	8670
ligands	9
Protein residues	1179
RMS (bonds)	0.002
RMS (angles)	0.46
Ramachandran favored (%)	98.29
Ramachandran allowed (%)	1.71
Ramachandran outliers (%)	0.00
Rotamer outliers (%)	0.00
Clashscore	5.49
Average B-factor	132.82
macromolecules	132.86
ligands	96.02
Number of TLS groups	6

Statistics for the highest-resolution shell are shown in parentheses.

Appendix Table S5: Populations obtained from Gaussian fitting of time-averaged distributions. *Related to Figure 2 and Appendix Figures S3 and S4.*

Apo	low E_{FRET} (0.4)	Intermediate E_{FRET} (0.6)	High E_{FRET} (0.9)
WT	0.73	0.19	0.08
M269A	0.71	0.26	0.03
G226L	0.42	0.35	0.23
Y204L	0.71	0.26	0.23
A345V	0.61	0.24	0.15
V366A	0.64	0.19	0.17
A345V V366A	0.80	0.16	0.03
Y204L A345V V366A	0.67	0.22	0.11
K290A	0.49	0.49	0.02
Y204L K290A	0.56	0.38	0.06
K290A A345V V366A	0.62	0.26	0.12
Y204L K290A A345V V366A	0.55	0.41	0.05
R276S M395R	0.31	0.68	0.01
Na^+/L-Asp-bound	low E_{FRET} (0.4)	Intermediate E_{FRET} (0.6)	High E_{FRET} (0.9)
WT	0.81	0.12	0.07
M269A	0.84	0.16	0.03
G226L	0.54	0.16	0.30
Y204L	0.77	0.15	0.08
A345V	0.65	0.13	0.22
V366A	0.63	0.13	0.23
A345V V366A	0.80	0.16	0.04
Y204L A345V V366A	0.70	0.20	0.10
K290A	0.59	0.27	0.13
Y204L K290A	0.56	0.26	0.17
K290A A345V V366A	0.63	0.23	0.14
Y204L K290A A345V V366A	0.66	0.26	0.08
R276S M395R	0.66	0.08	0.25

Appendix Figures

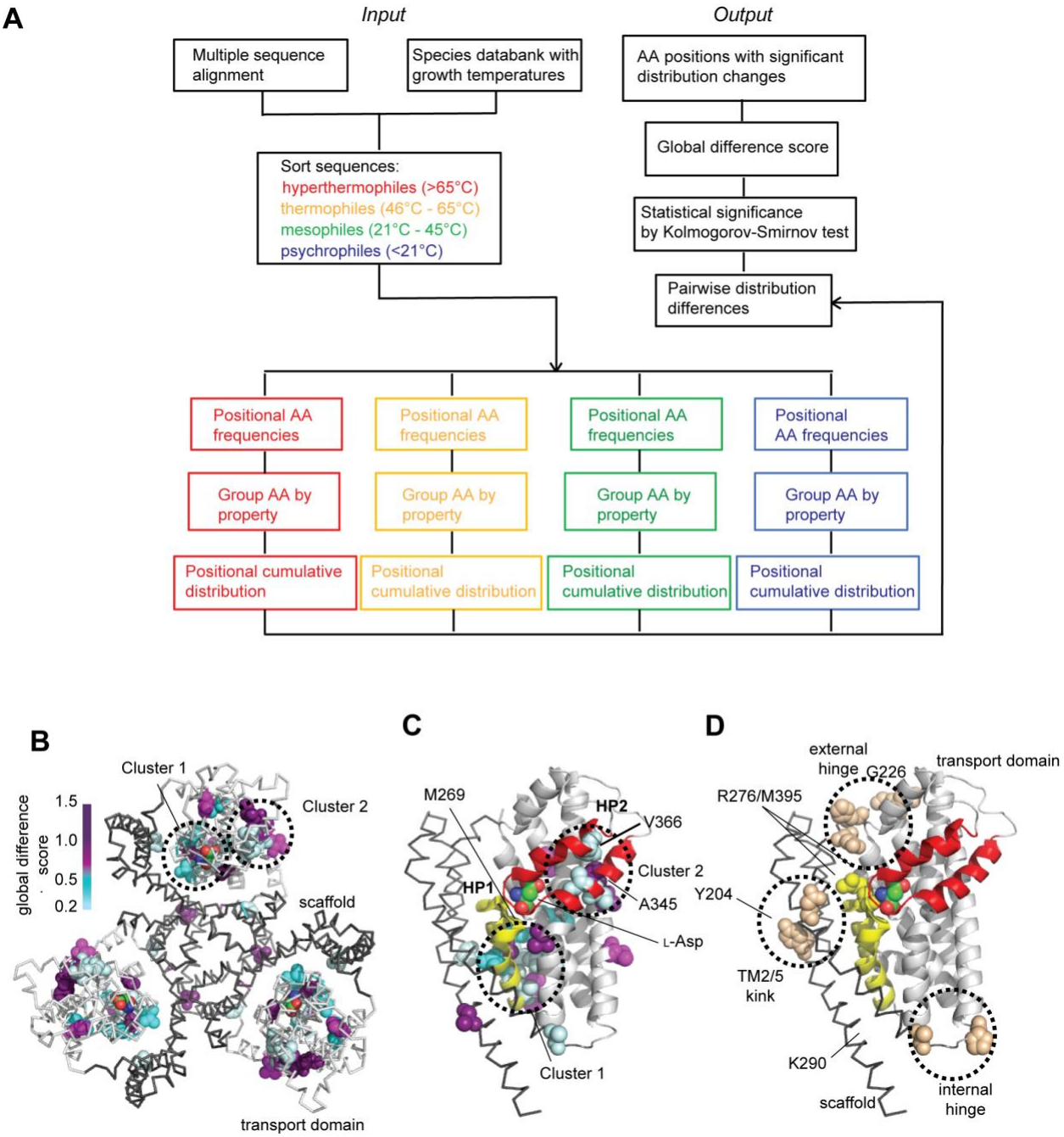

Appendix Figure S1: Bioinformatics analysis to identify gain-of-function mutations. *Related to Figure 1.* (**A**) Sequence analysis workflow. (**B**) Clusters of amino acids showing changes in the sidechain volume and/or physicochemical properties correlated with the optimal growth temperature of their species of origin. The Glt_{Ph} trimer is viewed from the extracellular side of the membrane and is shown in ribbon representation with the scaffold domain colored black and the

transport domain colored light gray. L-Asp molecules are shown as spheres and colored according to atom type. Residues with positive global difference scores are shown as spheres and colored according to the score with the scale bar shown on the left. Dotted lines emphasize two apparent clusters in one protomer. (**C**) A single protomer viewed in the membrane plane with the transport domain shown in cartoon representation and HP1 and HP2 colored yellow and red, respectively. Substrate and candidate residues are shown as spheres and colored as in B. TM4 is removed for clarity. Dotted circles have ~10 Å diameter. (**D**) A single protomer as in C, highlighting additional mutation sites, chosen based upon structural considerations.

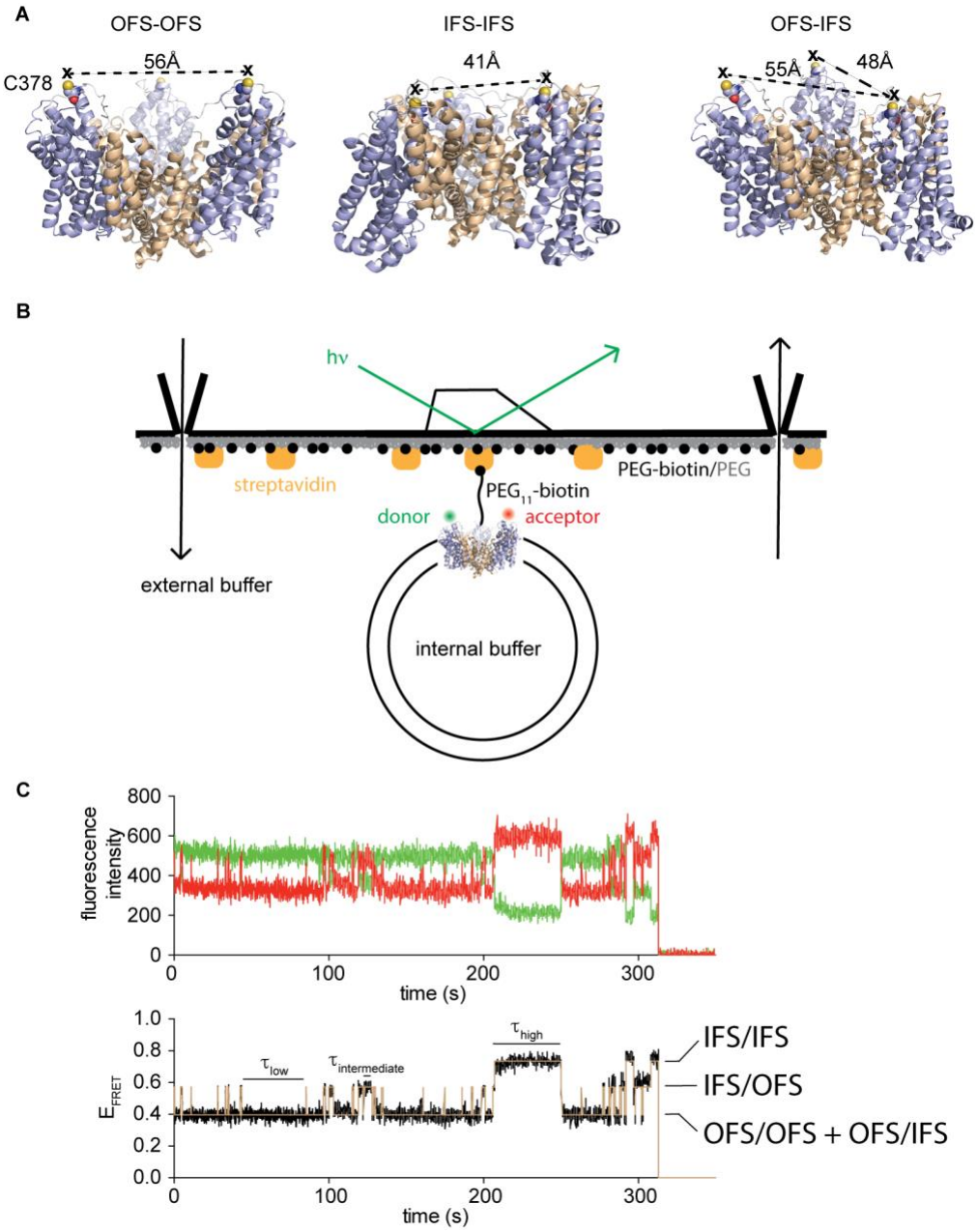

Appendix Figure S2: smFRET experimental setup. *Related to Figure 2.* (**A**) Cartoon representations of the Glt_{Ph} trimer. The labeling residue N378C is highlighted as spheres. Inter-subunit cysteine-to-cysteine distances are shown for the OFS (left), the IFS (middle), and an asymmetric trimer with two protomers in the OFS and the third in the IFS (right). Note that in the latter case, only isomerization of a protomer relative to its counter-clock neighbor gives rise to a measurable distance change. (**B**) smFRET TIRF microscopy setup with perfusion system. (**C**) An example smFRET trajectory. Anticorrelated changes of the donor and acceptor fluorophore

emissions (top) are converted into FRET efficiencies (bottom, black) and idealized assuming three FRET efficiency (E_{FRET}) states (brown) corresponding to protomer configurations shown in A.

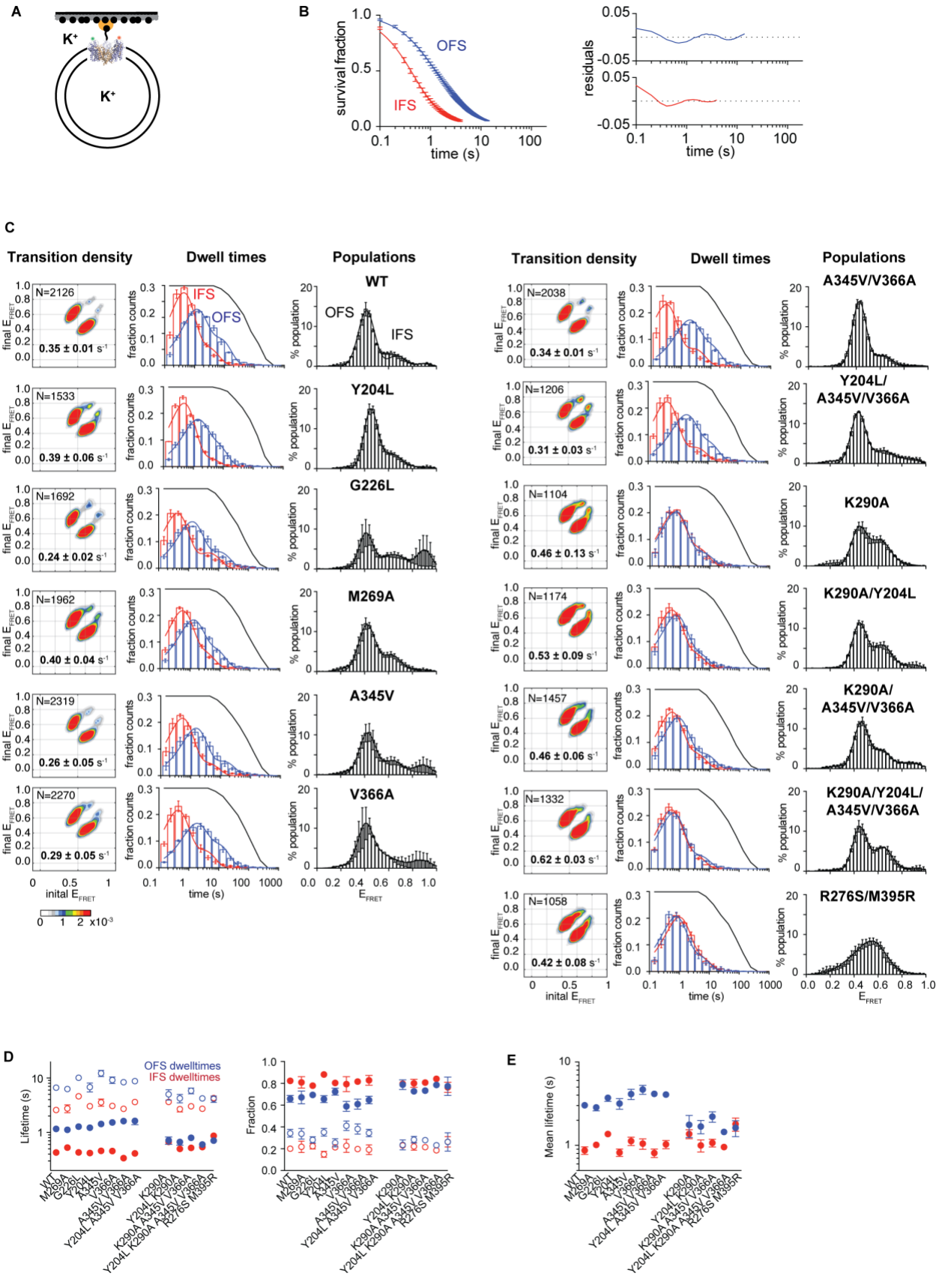
A
K+
K+
B
survival fraction
OFS
IFS
time (s)
residuals
time (s)
C
Transition density
Dwell times
Populations
WT
N=2126
0.35 ± 0.01 s-1
Y204L
N=1533
0.39 ± 0.06 s-1
G226L
N=1692
0.24 ± 0.02 s-1
M269A
N=1962
0.40 ± 0.04 s-1
A345V
N=2319
0.26 ± 0.05 s-1
V366A
N=2270
0.29 ± 0.05 s-1
A345V/V366A
N=2038
0.34 ± 0.01 s-1
Y204L/ A345V/V366A
N=1206
0.31 ± 0.03 s-1
K290A
N=1104
0.46 ± 0.13 s-1
K290A/Y204L
N=1174
0.53 ± 0.09 s-1
K290A/ A345V/V366A
N=1457
0.46 ± 0.06 s-1
K290A/Y204L/ A345V/V366A
N=1332
0.62 ± 0.03 s-1
R276S/M395R
N=1058
0.42 ± 0.08 s-1
final EFRET
fraction counts
% population
inital EFRET
time (s)
EFRET
0 1 2 x10-3
D
OFS dwelltimes
IFS dwelltimes
Lifetime (s)
Fraction
WT
M269A
G226L
Y204L
A345V
V366A
A345V V366A
Y204L A345V V366A
K290A
K290A A345V V366A
Y204L K290A A345V V366A
R276S M395R
E
Mean lifetime (s)

Appendix Figure S3: Transport domain dynamics of the apo Glt_{Ph}. *Related to Figure 2.* (**A**) Representation of the experimental setup. (**B**) Survival plots of the OFS and the IFS of WT Glt_{Ph} fitted to double exponentials with residuals shown on the right. (**C**) The following plots are shown for each Glt_{Ph} variant. Left panels: transition density plots. Shown on each panel are the number of trajectories analyzed (*N*) and the population-wide mean transition frequency calculated as the ratio of the total number of transitions and the total trajectory lifetime. Scalebar is at the bottom. Middle panels: dwell-time distributions of the OFS in blue and the IFS in red. Thin lines through the data are fits to biexponential probability density functions. Black lines are the survivals of the FRET lifetimes normalized between 1 and 0. Right panels: time-averaged population distributions of E_{FRET} fitted to three Gaussian distributions with mean E_{FRET} values of ~0.4, 0.6 and 0.9; (**D**) Lifetimes (left) and component fractions (right) for the OFS (blue) and the IFS (red) obtained by fitting dwell-time distributions in C. Open and filled symbols represent the long and short lifetime components, respectively. (**E**) Mean OFS and IFS lifetimes calculated using fitted parameters from D. Data are averages and standard errors of at least three independent measurements.

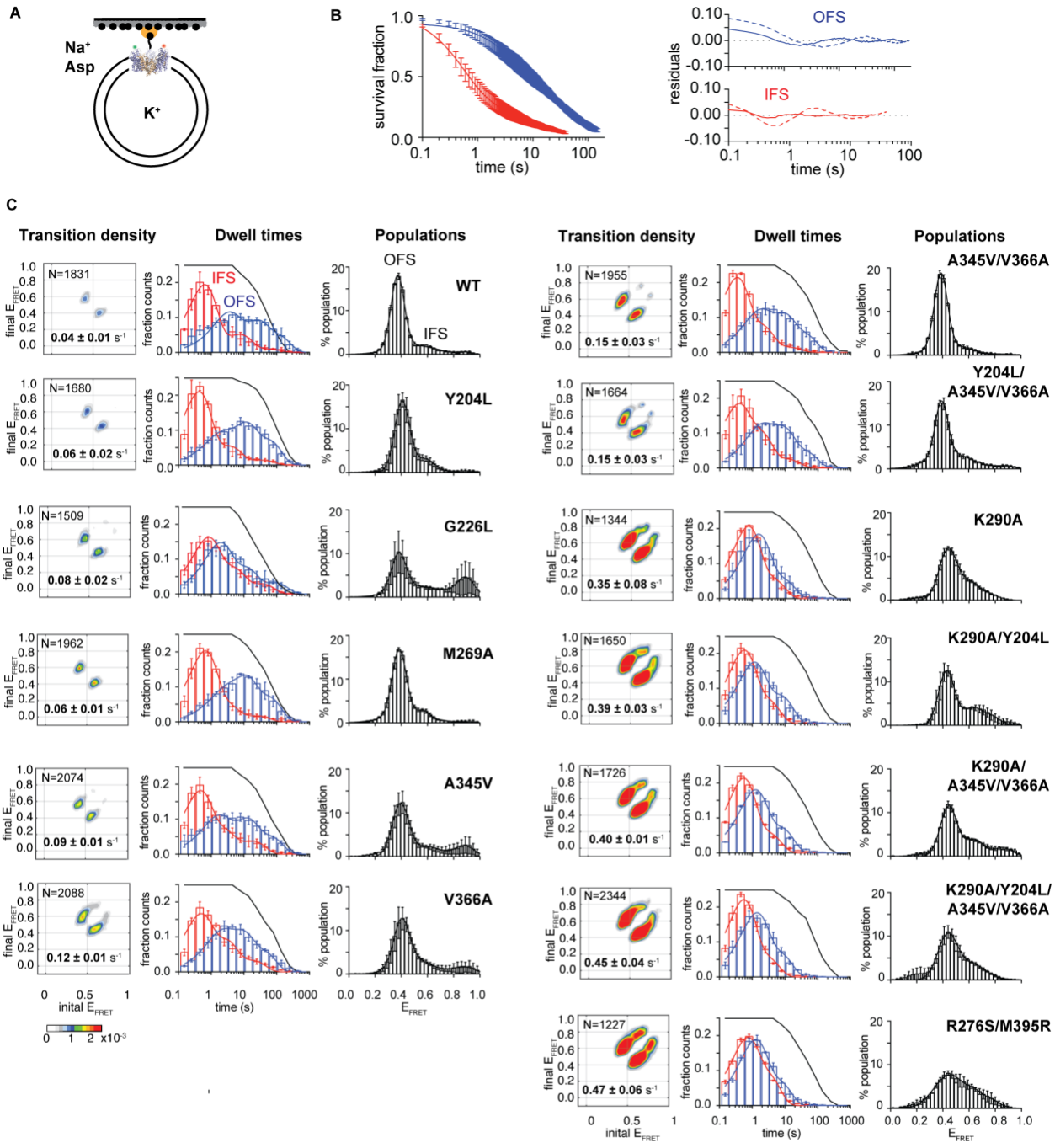
A
Na+
Asp
K+
B
survival fraction
time (s)
OFS
IFS
residuals
C
Transition density
Dwell times
Populations
WT
Y204L
G226L
M269A
A345V
V366A
A345V/V366A
Y204L/
A345V/V366A
K290A
K290A/Y204L
K290A/
A345V/V366A
K290A/Y204L/
A345V/V366A
R276S/M395R
final E_FRET
fraction counts
% population
inital E_FRET
E_FRET
0.04 ± 0.01 s-1
0.06 ± 0.02 s-1
0.08 ± 0.02 s-1
0.06 ± 0.01 s-1
0.09 ± 0.01 s-1
0.12 ± 0.01 s-1
0.15 ± 0.03 s-1
0.35 ± 0.08 s-1
0.39 ± 0.03 s-1
0.40 ± 0.01 s-1
0.45 ± 0.04 s-1
0.47 ± 0.06 s-1
N=1831
N=1680
N=1509
N=1962
N=2074
N=2088
N=1955
N=1664
N=1344
N=1650
N=1726
N=2344
N=1227
D
OFS dwelltimes
IFS dwelltimes
Lifetime (s)
Fraction
E
Mean lifetime (s)

Appendix Figure S4: Transport domain dynamic under transport conditions. *Related to Figure 2.* (**A**-**E**) Panels are as in Appendix Figure S3. In B, data are fitted to triple exponentials with residuals shown on the right. Dashed lines correspond to residuals of the double exponential fits. In C, dwell-time distributions were fitted to tri-exponential probability density functions for mutants that do not contain K290A or R276S/M395R mutations. The dwell-time distributions of the latter were fitted to biexponential probability density functions. In D, crossed, open, and solid symbols correspond to long, intermediate, and short lifetimes, respectively.

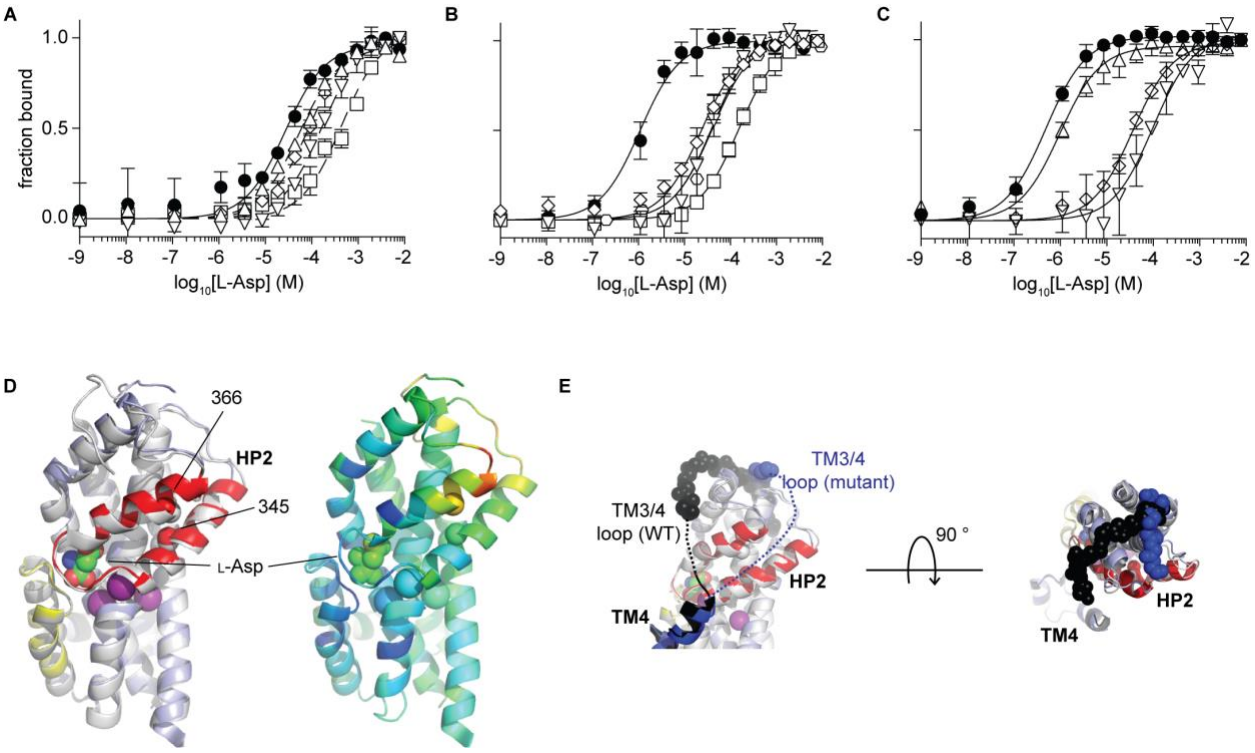

Appendix Figure S5: L-Asp affinity of the Glt$_{Ph}$ variants. *Related to Figure 3.* (**A-C**) L-Asp binding isotherms measured at 25 °C in the presence of 1 mM Na^+ (**A**) or 10 mM Na^+ (**B** and **C**). Lines represent fits to the Hill equation with n = 1. In A: WT (filled circles), Y204L (triangles), G226L (diamonds), M269A (downward triangles), A345V (squares). In B: WT (filled circles), V366A (squares), A345V/V366A (triangles), Y204L/A345V/V366A (diamonds), R276S/M395R (hexagons). In C: K290A (filled circles), Y204L/K290A (triangles), K290A/A345V/V366A (downward triangles), Y204L/K290A/A345V/V366A (diamonds). (**D**) Superposition of the transport domains of the Y204L/A345V/V366A mutant and WT Glt$_{Ph}$ (PDB accession code: 2NWX). The structures are colored as in Figure 3 (left) and Y204L/A345V/V366A Glt$_{Ph}$ from low (blue) to high (orange) B-factors (right). Location of residues 345 and 366 are highlighted by depicting their Cα atoms as spheres. (**E**) Close-up of the resolved N-terminal section of the TM3/4-loop by superposition of the transport domains of Y204L/A345V/V366A mutant and the WT Glt$_{Ph}$ (PDB accession code: 2NWX).

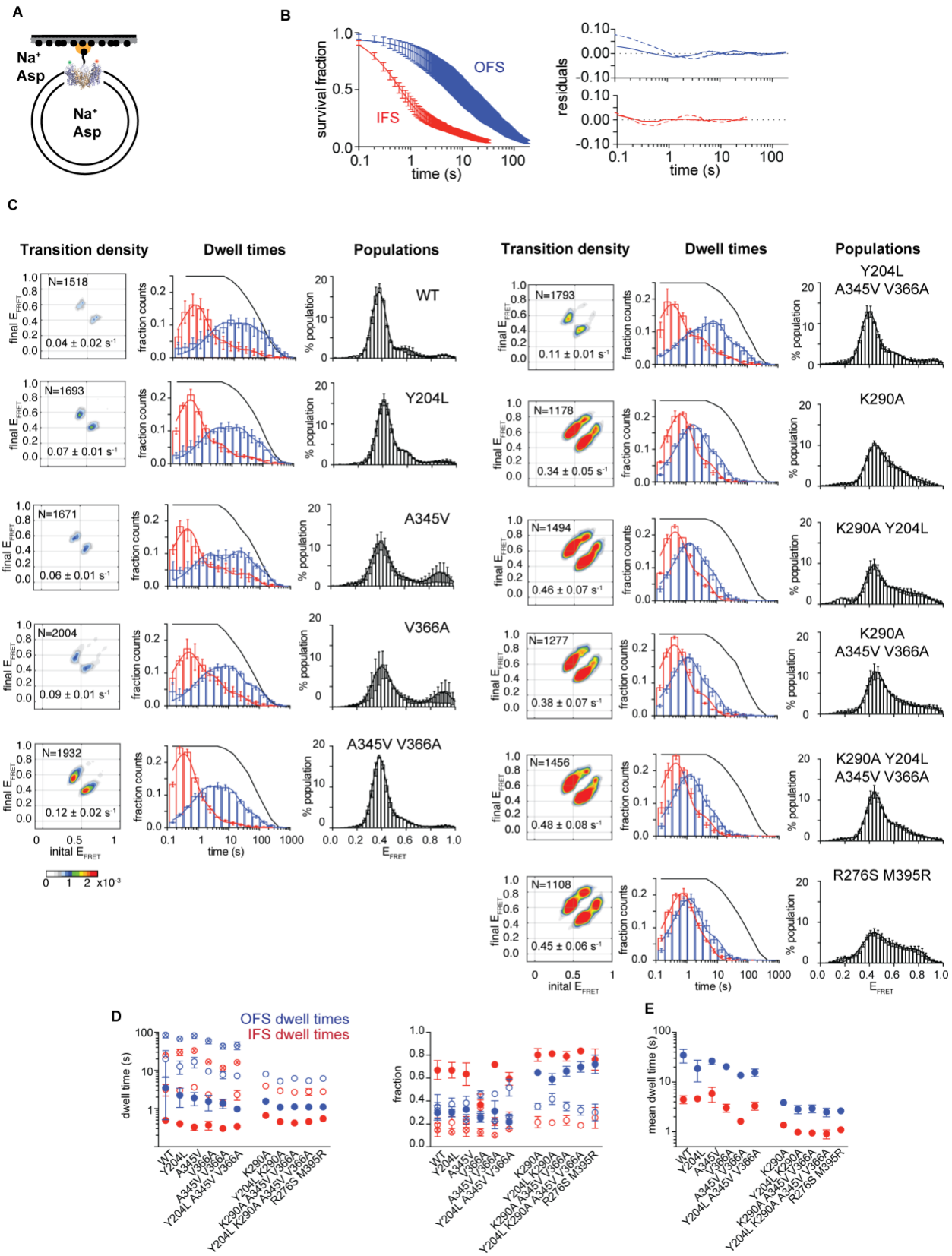
A
Na+
Asp
Na+
Asp
B
survival fraction
OFS
IFS
time (s)
residuals
time (s)
C
Transition density
Dwell times
Populations
N=1518
0.04 ± 0.02 s-1
WT
N=1693
0.07 ± 0.01 s-1
Y204L
N=1671
0.06 ± 0.01 s-1
A345V
N=2004
0.09 ± 0.01 s-1
V366A
N=1932
0.12 ± 0.02 s-1
A345V V366A
N=1793
0.11 ± 0.01 s-1
Y204L
A345V V366A
N=1178
0.34 ± 0.05 s-1
K290A
N=1494
0.46 ± 0.07 s-1
K290A Y204L
N=1277
0.38 ± 0.07 s-1
K290A
A345V V366A
N=1456
0.48 ± 0.08 s-1
K290A Y204L
A345V V366A
N=1108
0.45 ± 0.06 s-1
R276S M395R
final EFRET
fraction counts
% population
inital EFRET
time (s)
EFRET
0 1 2 x10-3
D
OFS dwell times
IFS dwell times
dwell time (s)
fraction
E
mean dwell time (s)
WT
Y204L
A345V
V366A
A345V V366A
Y204L A345V V366A
K290A
Y204L K290A
K290A A345V V366A
Y204L K290A A345V V366A
R276S M395R

Appendix Figure S6: Transport domain dynamics under symmetric conditions in the presence of 200 mM Na^+ ions and 100 µM L-Asp. *Related to Figures 4 and 5.* (**A-E**) Panels are as in Appendix Figure S4.

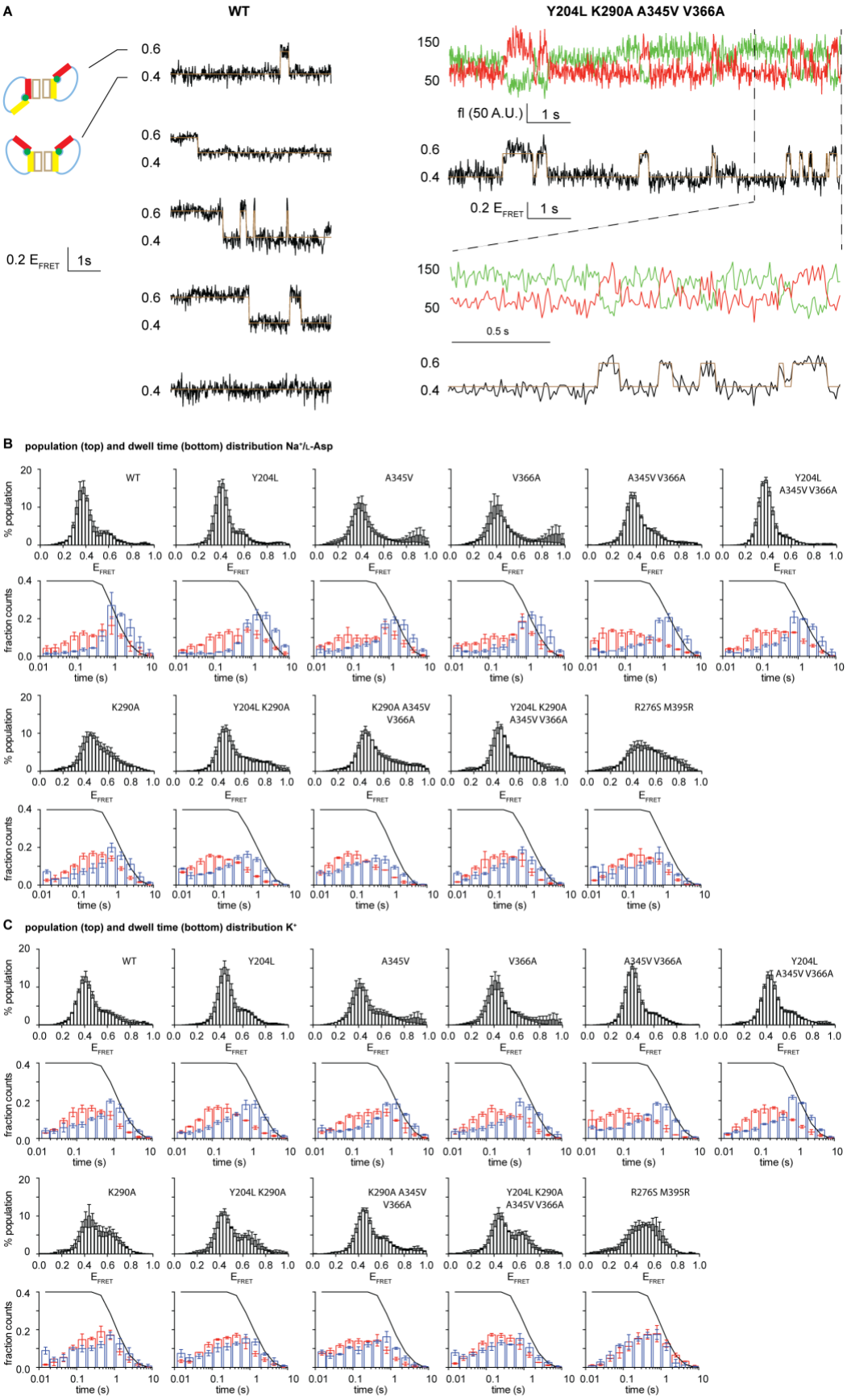
A
WT
Y204L K290A A345V V366A
0.2 E_FRET
1s
fl (50 A.U.)
1 s
0.2 E_FRET
1 s
0.5 s
B
population (top) and dwell time (bottom) distribution Na+/L-Asp
WT
Y204L
A345V
V366A
A345V V366A
Y204L A345V V366A
K290A
Y204L K290A
K290A A345V V366A
Y204L K290A A345V V366A
R276S M395R
% population
fraction counts
E_FRET
time (s)
C
population (top) and dwell time (bottom) distribution K+

Appendix Figure S7: Transport domain dynamics measured at 10 ms time resolution. *Related to Figure 4* **(A)** Representative single-molecule trajectories. Raw E_{FRET} data are black, idealizations are brown, donor and acceptor fluorescence intensities are green and red, respectively. Scale bar and the conformational states corresponding to the low and intermediate E_{FRET} values are on the left. Data are shown for WT Glt_{Ph} and the most performant gain-of-function mutant, as indicated above the panels. In **(B)** and **(C)** the time-averaged population distributions (top) and dwell-time distributions of the OFS in blue and the IFS in red (bottom) are shown for each Glt_{Ph} mutant under symmetric conditions in the presence of 200 mM Na^+ ions and 100 µM L-Asp, and under apo conditions in the presence of 200 mM K^+ ions, respectively. Black lines are the survivals of the FRET lifetimes normalized between 1 and 0.

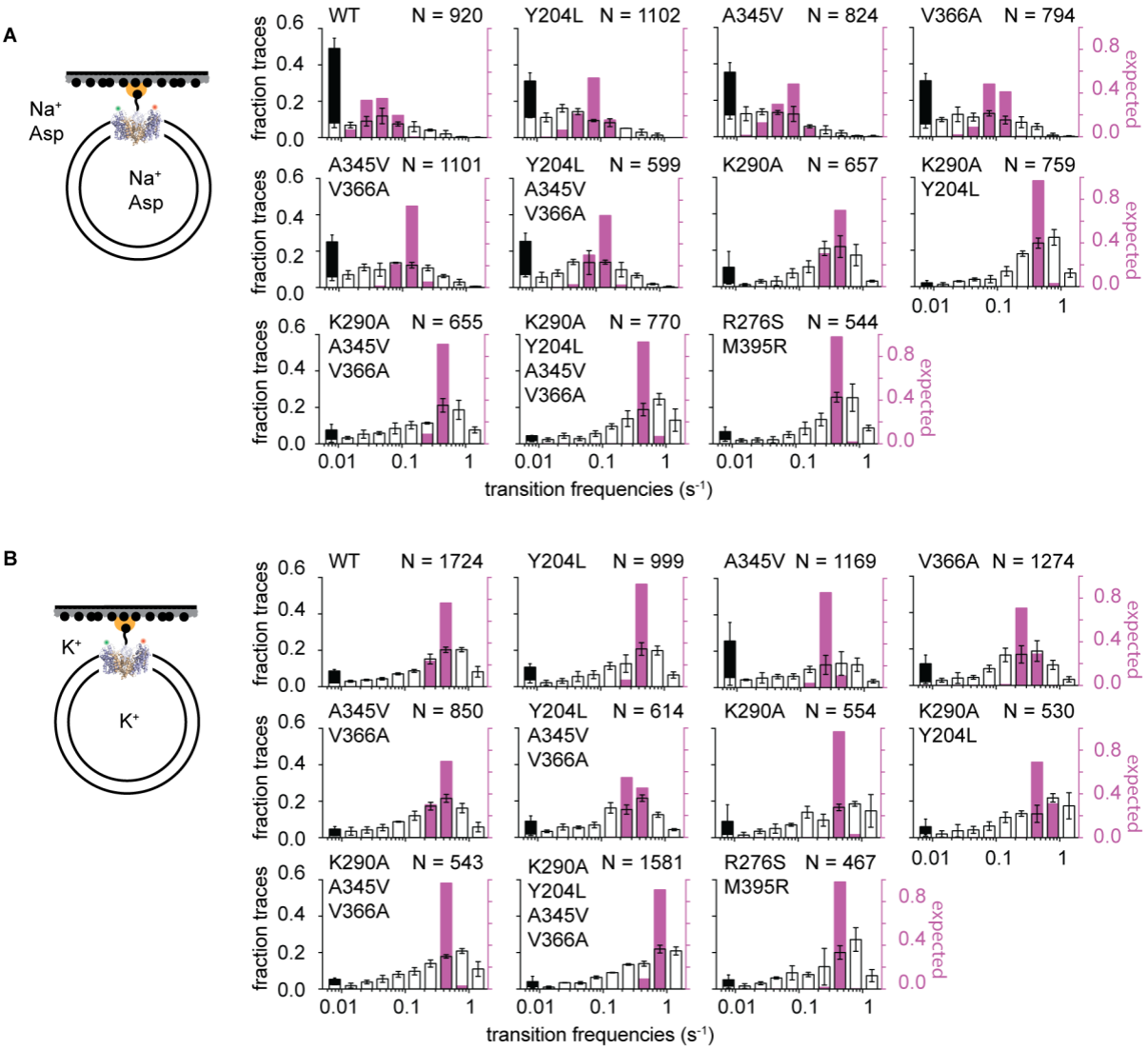

Appendix Figure S8: Distributions of transition frequencies of individual trajectories in the presence of symmetric 200 mM Na^+ ions and 100 µM L-asp (A) and under apo conditions (B). *Related to Figure 4.* The open bars show the transition frequency distributions of Glt_{Ph} molecules with at least one observed transition. The stacked black bars show the fractions of the trajectories without observed transitions. The pink bars show the expected binomial distributions calculated, assuming that all trajectories share the same mean transition frequency reported in Appendix Figure S6. The number of trajectories included in the analysis, *N* is shown on each panel. Data are shown as averages and standard errors of three independent experiments.

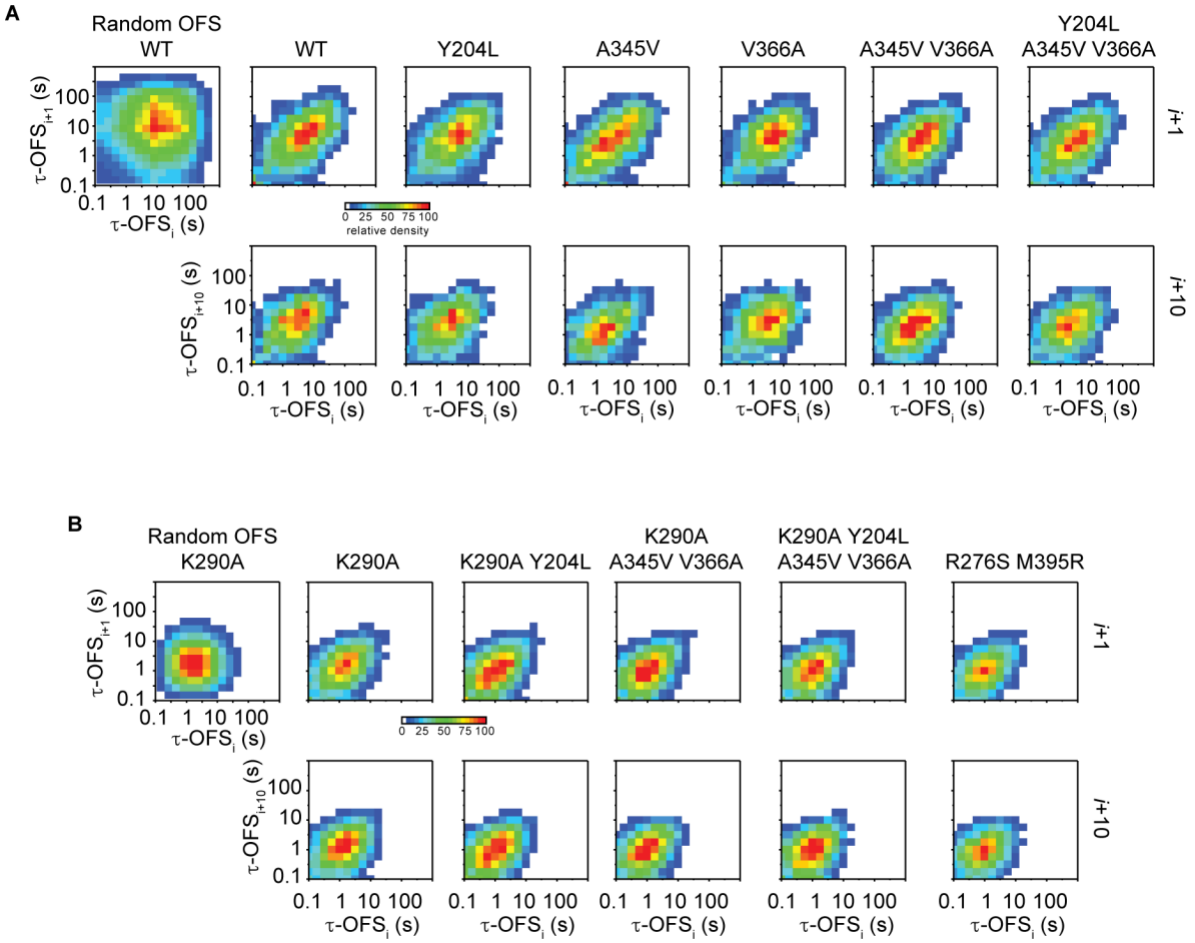

Appendix Figure S9: Correlated durations of sequential OFS dwells in Glt$_{Ph}$ variants. *Related to Figure 4.* 2D histograms of durations of two consecutive OFS dwells (top row) and two OFS dwells separated by 10 visitations to the state (bottom row) are shown for less (**A**) and more (**B**) dynamic Glt$_{Ph}$ variants. Histograms expected for random uncorrelated dwells are shown on the left for the WT Glt$_{Ph}$ (**A**) and the K290A mutant (**B**). Characteristic elongated shapes of the experimental histograms are due to correlations between the lengths of the dwells.

A

Glt_{Ph} variant	% traces OFS	% traces IFS
WT	95 ± 1	97 ± 1
Y204L	88 ± 2	94 ± 1
A345V	90 ± 5	95 ± 2
V366A	89 ± 1	94 ± 2
A345V V366A	89 ± 2	92 ± 1
Y204L A345V V366A	83 ± 1	89 ± 1
K290A	82 ± 7	87 ± 2
K290A Y204L	86 ± 3	88 ± 1
K290A A345V V366A	86 ± 2	88 ± 2
K290A Y204L A345V V366A	86 ± 1	88 ± 2
R276S M395R	81 ± 2	88 ± 1

B

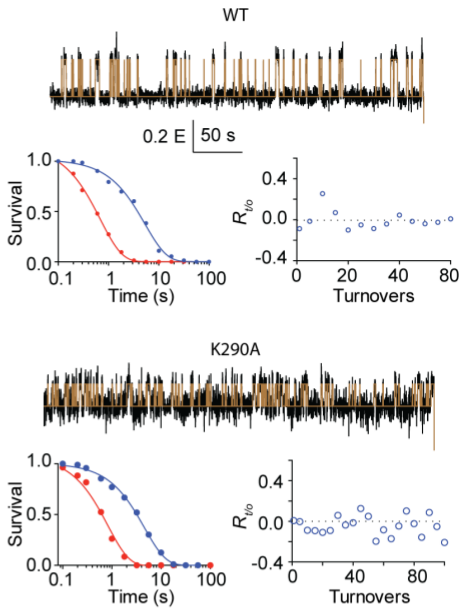

C

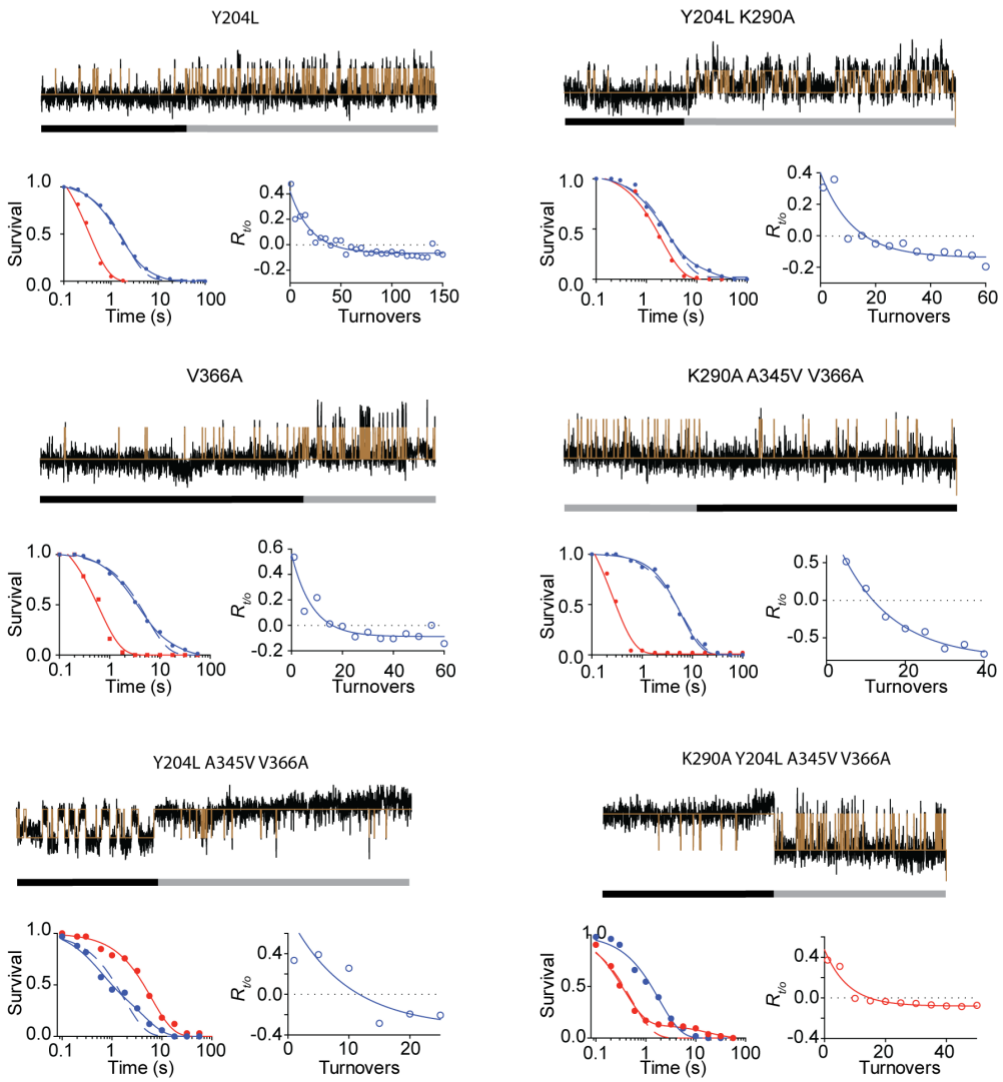

Appendix Figure S10: Mode switching. *Related to Figure 4.* (**A**) Fractions of kinetically homogeneous traces for which the survival of the OFS and IFS dwell times fit well to single exponential functions. (**B**) Examples of kinetically homogeneous single-molecule trajectories recorded for the WT Glt_{Ph} and the K290A mutant in the presence of 200 mM Na^+ ions and 100 µM L-Asp. Below each trajectory, shown are the survival plots for the OFS (blue) and the IFS (red) fitted to single exponential functions and the plots of autocorrelation coefficients, $R_{t/o}$, fluctuating around 0. (**C**) Traces showing mode switching. Black and grey bars below the trajectories indicate apparent slow and fast modes. For these traces, fitting the survival plots of either the OFS, IFS or both to double exponential functions (solid lines) improves the coefficient of determination over 5 % compared to single exponentials (dotted lines). Autocorrelation functions reflect temporal segregation of the similar dwells. Solid lines are fits to single exponentials to guide the eye.

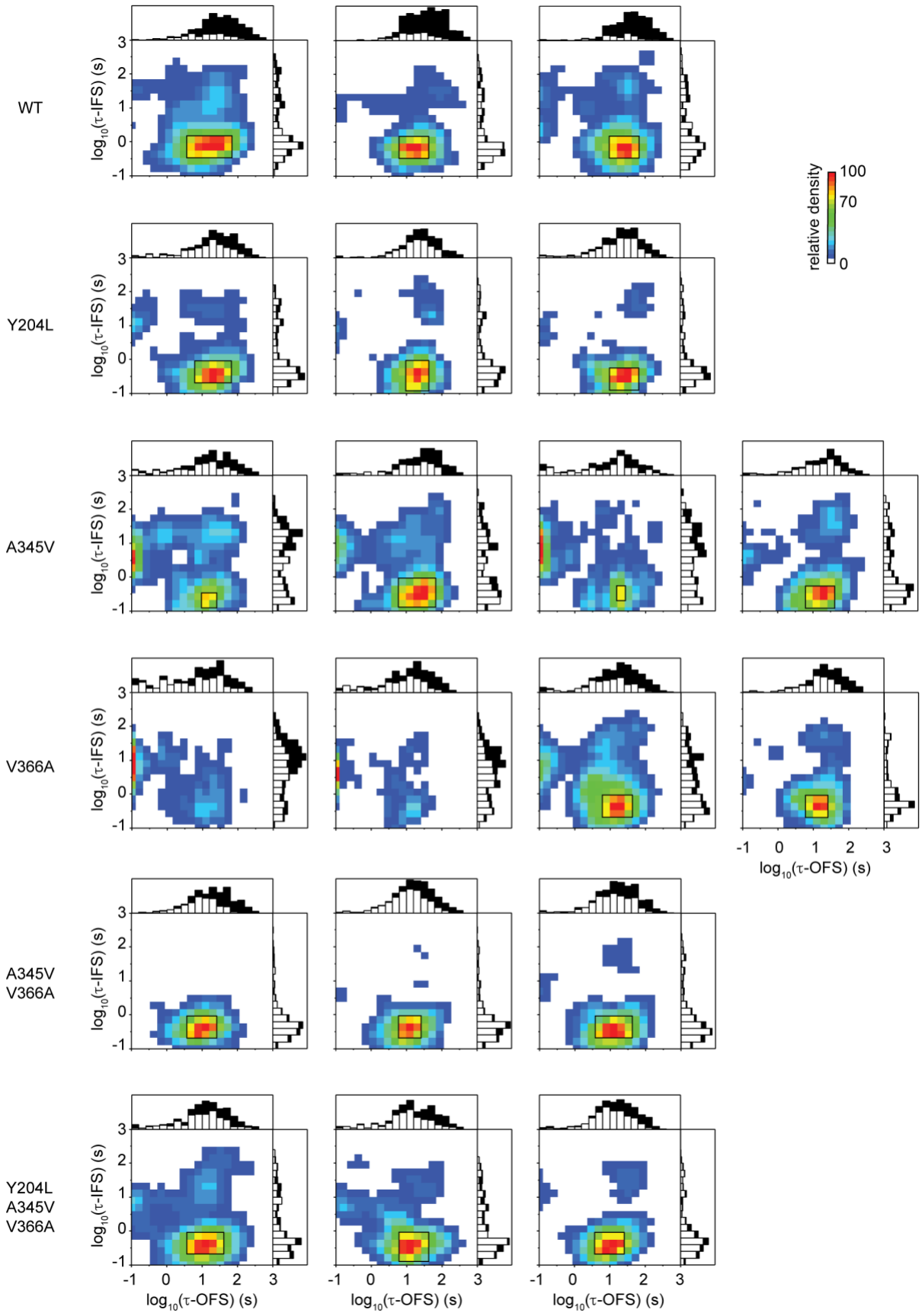
WT
Y204L
A345V
V366A
A345V
V366A
Y204L
A345V
V366A
log10(τ-IFS) (s)
log10(τ-OFS) (s)
relative density
100
70
0

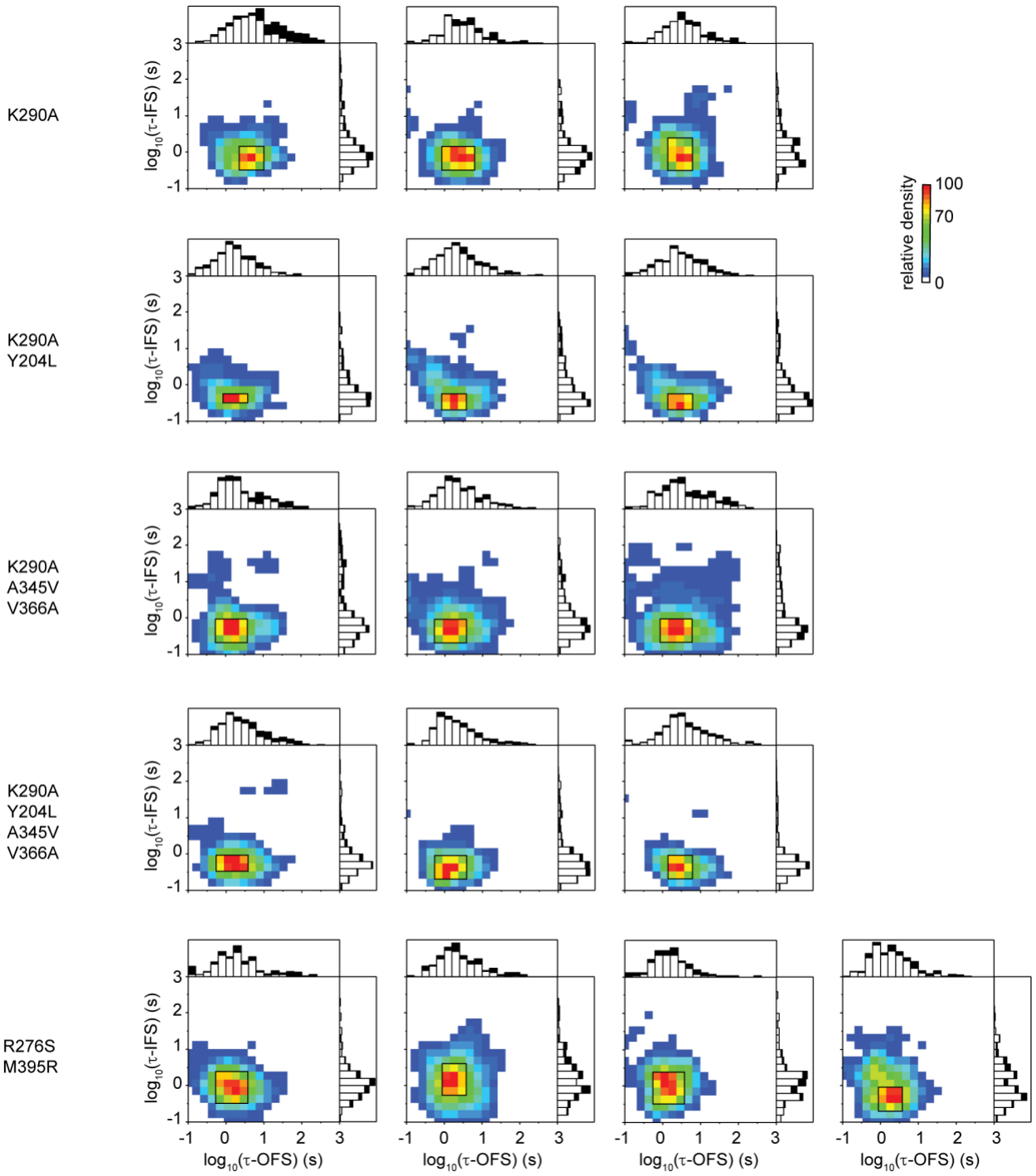

Appendix Figure S11: Distributions of the OFS and IFS lifetime pairs for individual molecules per experimental repeat in 200 mM Na^+ ions and 100 µM L-Asp. *Related to Figure 6.* 2D-histograms of lifetime pairs obtained for trajectories exhibiting single exponential behavior. Scale bar shows relative density normalized by the number of molecules. Above and to the right

of each panel are stacked histograms of, respectively, the OFS and IFS lifetimes of the analyzed molecules (open bars), and the photobleaching times of molecules with no observed transitions (black bars). A box highlights the molecules selected for the determination of the OFS and IFS lifetimes (termed typical mode).

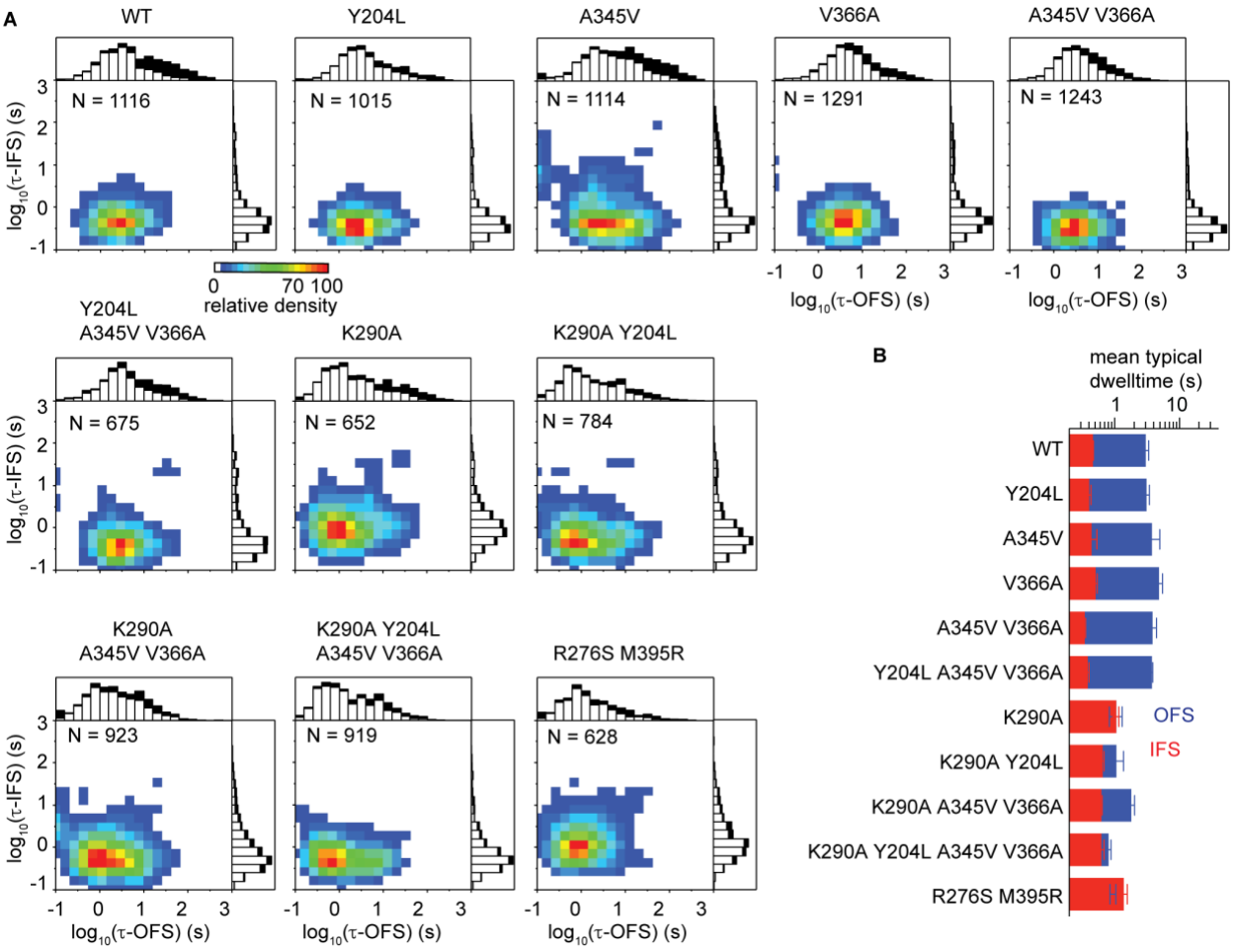

Appendix Figure S12: Distributions of the OFS and IFS lifetime pairs for individual molecules under apo conditions. *Related to Figure 6.* **(A)** 2D histograms of the OFS and IFS lifetime pairs obtained for all trajectories exhibiting single exponential behavior of the survival plots. The number of traces *N*, pooled together from at least three independent experiments, is shown on each panel. Stacked histograms of the mean lifetimes (open bars) and the photobleaching times of the molecules with no observed transitions (black bars) are shown above and to the right of the panels for the OFS and IFS, respectively. Scale bar shows relative density normalized to the number of molecules included (*N*). (**B**) Mean lifetimes of the molecules falling within 30 % of the most populated bins of the 2D-histograms (yellow to red). Data are shown as means and standard errors of three independent measurements.

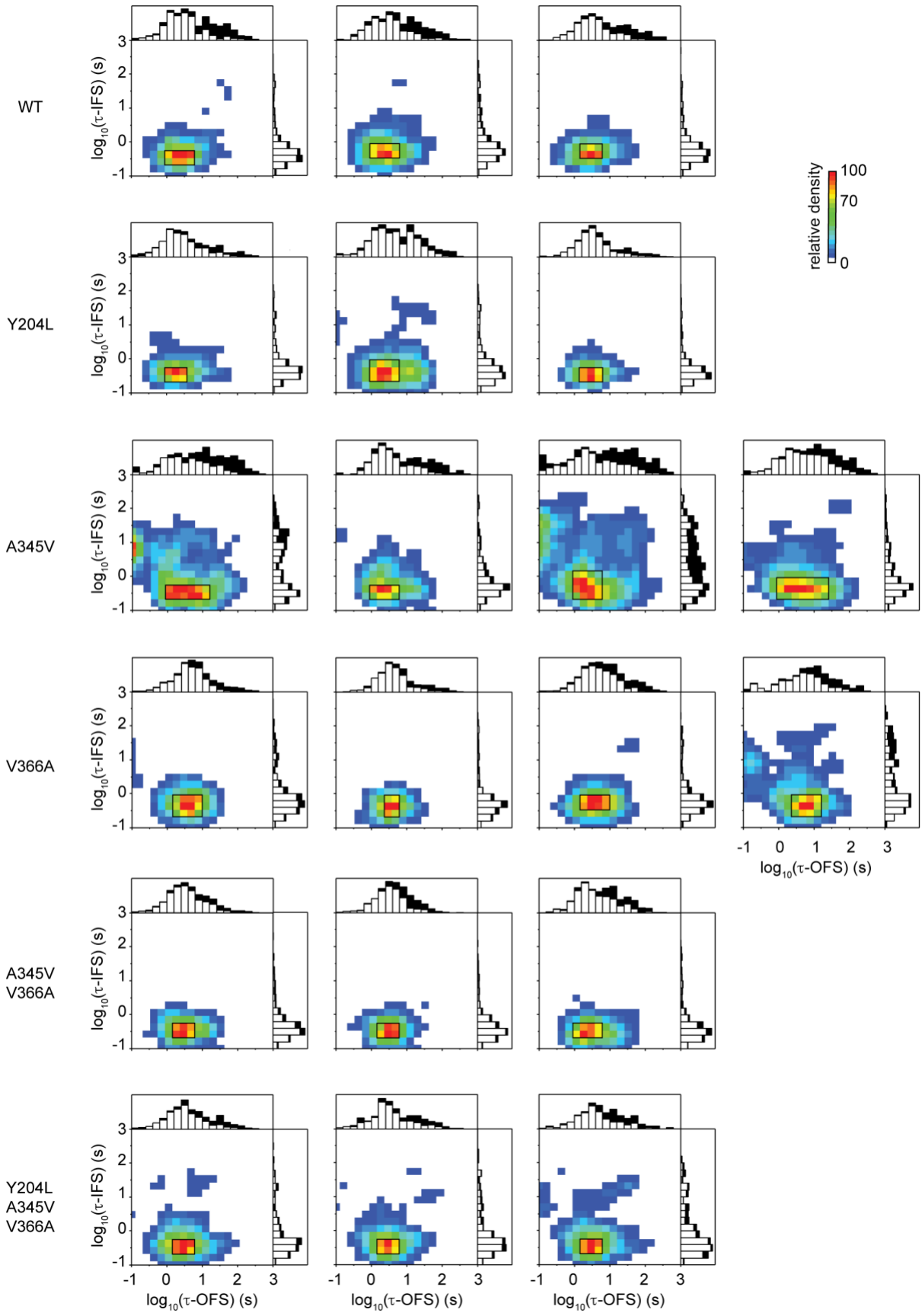
WT
Y204L
A345V
V366A
A345V
V366A
Y204L
A345V
V366A
log10(τ-IFS) (s)
log10(τ-OFS) (s)
relative density
100
70
0

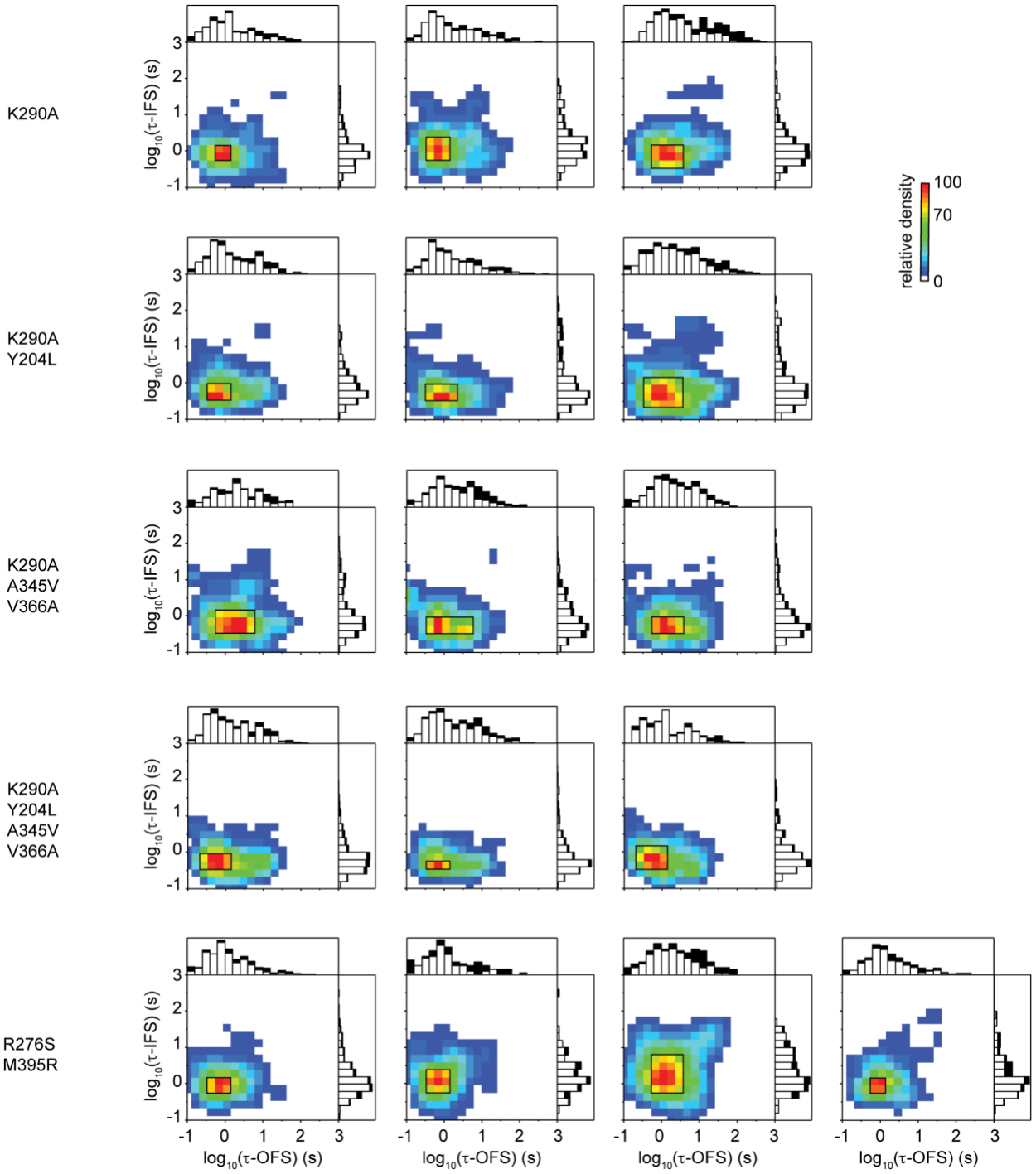

Appendix Figure S13: Distributions of the OFS and IFS lifetime pairs for individual molecules per experimental repeat under apo conditions. *Related to Figure 6.* 2D histograms of the OFS and IFS lifetime pairs obtained for all trajectories exhibiting single exponential behavior of the survival plots. Data are presented as in Appendix Figure S11.

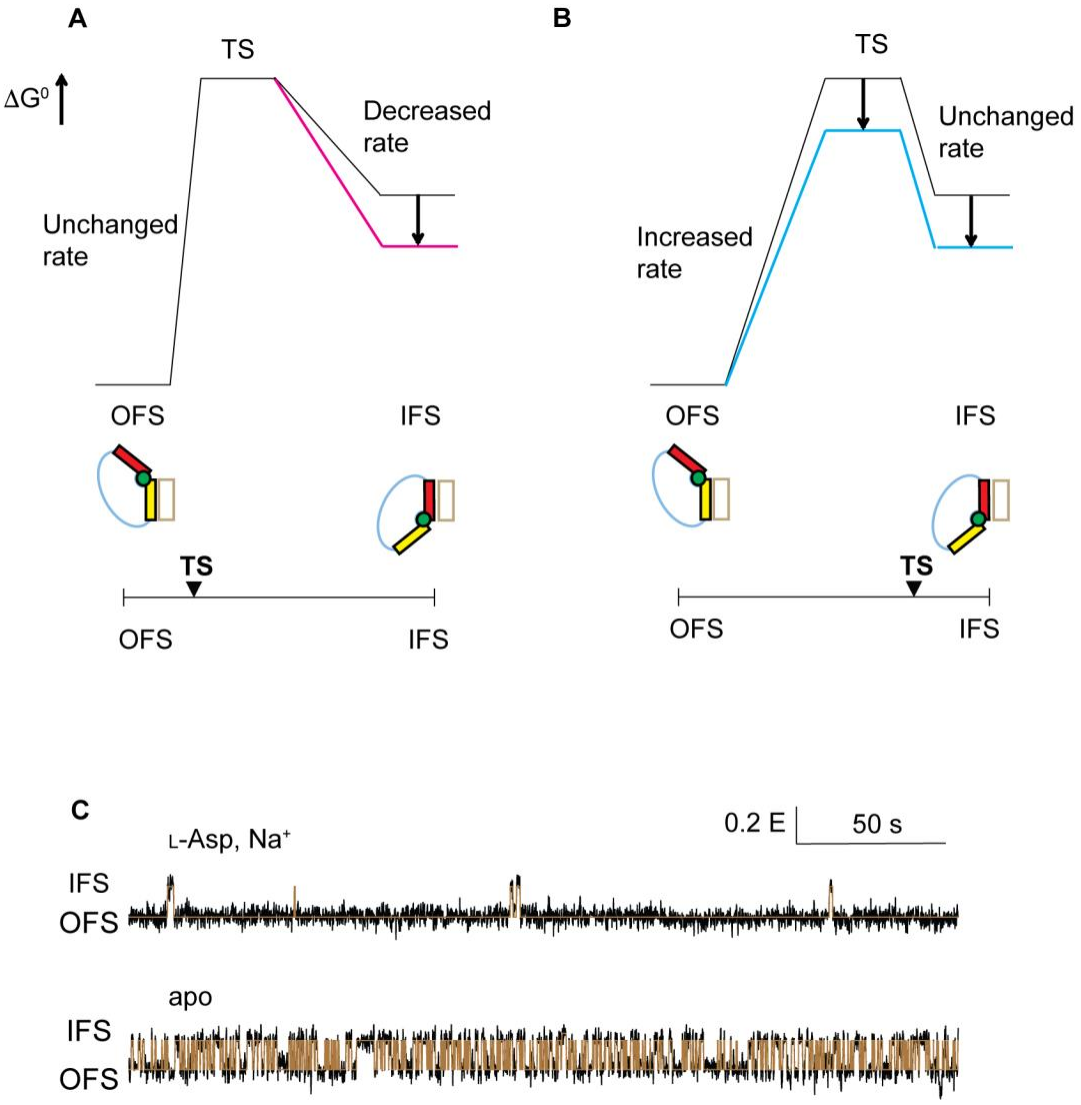

Appendix Figure S14: Transition state analysis. *Related to Figure 6.* (**A, B**) Free energy diagram of the OFS to IFS conformation change (black) and the expected effect of perturbations (colors) if the TS is similar to the OFS (**A**) or the IFS (**B**). Cartoon representations of the low-energy states are below the diagrams. (**C**) Representative smFRET trajectories for WT Glt_{Ph} bound to L-Asp and Na^+-ions (top) and in the absence of ligands (bottom). The scale bar is on the upper right of the panel.